sustainability

MDPI

Article

Synthesis and Recyclability of Sheet-like Cobalt Carbonate Recovered from Spent Li-Ion Batteries Using a Simple Hydrometallurgy Process

Abdelhay Aboulaich *, Afaf Yaden, Nabil Elhalya, Marwa Tayoury, Mohamed Aqil, Loubna Hdidou, Mouad Dahbi and Jones Alami

Materials Science, Energy and Nano-Engineering Department, Mohammed VI Polytechnic University (UM6P), Lot 660, Hay Moulay Rachid, Bengurir 43150, Morocco; afaf.yaden@um6p.ma (A.Y.); nabil.elhalya@um6p.ma (N.E.); marwa.tayoury@um6p.ma (M.T.); mohamed.aqil@um6p.ma (M.A.); loubna.hdidou@um6p.ma (L.H.); mouad.dahbi@um6p.ma (M.D.); jones.alami@um6p.ma (J.A.)

* Correspondence: abdelhay.aboulaich@um6p.ma; Tel.: +212-6-00-83-20-11

Abstract: In the present manuscript, a simple hydrometallurgy process for recovering and recycling cobalt from spent lithium cobalt oxide $LiCoO_2$ (LCO) in lithium-ion batteries (LIBs) is described. First, the black material (BM) containing LCO active material is extracted by discharging, dismantling and detachment of cathode active materials with an organic solvent. Then, sulfuric acid (H_2SO_4) and hydrogen peroxide (H_2O_2) are used to fully dissolve Co and Li in an aqueous solution at high dissolution efficiency (more than 99% of Li and Co). After a purification step, Co is selectively precipitated and separated from Li, as $CoCO_3$, using a simple method. Results show that the obtained $CoCO_3$ crystals have a unique sheets-like structure with a purity of more than 97% and could be reused to regenerate LCO active material for LIB. The as-prepared sheet-like $CoCO_3$ was then converted to flower-like LCO through a solid-state reaction with commercial lithium carbonate (Li_2CO_3). Electrochemical performances of the regenerated LCO (LCO_{Reg}) in LIB have been studied. Interestingly, the flower-like LCO_{Reg} showed a good charge capacity of about 145 $mAh.g^{-1}$ at the first cycle, compared to LCO synthesized from commercial cobalt and lithium precursors (LCO_{Com}). Specific charge capacity and columbic efficiency also remained relatively stable after 60 charge/discharge cycles. The proposed recycling process of Co in the present work doesn't require the use of the complicated and expensive solvent extraction method and thus it is simple, cost-effective, environmentally-friendly and could be used for recovering high purity critical metals such as Co and Li from spent LIBs at the industrial scale.

Keywords: recycling; Li-ion battery; cobalt carbonate; regenerated $LiCoO_2$; electrochemistry

Citation: Aboulaich, A.; Yaden, A.; Elhalya, N.; Tayoury, M.; Aqil, M.; Hdidou, L.; Dahbi, M.; Alami, J. Synthesis and Recyclability of Sheet-like Cobalt Carbonate Recovered from Spent Li-Ion Batteries Using a Simple Hydrometallurgy Process. *Sustainability* **2022**, *14*, 2552. https://doi.org/10.3390/su14052552

Academic Editor: Catherine Housecroft

Received: 6 January 2022
Accepted: 17 February 2022
Published: 23 February 2022

1. Introduction

The global rechargeable Lithium-Ion Batteries (LIBs) market was valued in 2020 around USD 40.5 billion and is expected to increase to about USD 92 billion by 2026 [1]. China dominates the LIB manufacturing market with the production of 4.8 billion LIBs units in 2013, and 18.85 billion LIBs units in 2020 [2]. Given that most LIBs have a life-span of around 1–3 years, a huge amount of obsolete and end-of-life LIBs enter the waste stream each year. For example, the total weight of discarded batteries in China alone was estimated to be higher than 500,000 tons in 2020 [3]. Expectations also predict that the growing electrical vehicles (EV) adoption will generate in the near future (2020–2040) around 300 million tons of end-of-life LIBs [4], which represents a real urban mine of strategic and critical metals such as Cobalt (Co), Lithium (Li) and Nickel (Ni). Among the valuable metals contained in these LIBs scraps, Co has high economic benefits because of its wide applications in magnets, super alloys, aircraft engines and LIBs. Its commercial value reached more than USD 61,000/t in November 2021, which is much higher than the

value of any other important industrial metal such as Cu (UDS 9850/t), Al (USD 2683/t), Zn (USD 3208/t), Pb (USD 2209/t) or Fe (USD 92/t) [5]. Therefore, recycled Co from cathode materials of spent LIBs could be reused to produce new LIBs or as cobalt precursor in other applications, which would generate a significant economic benefit. Co is also a scarce strategic metal that could be only extracted as a by-product of nickel and copper mining processes from natural ores. The fact that almost 70% of Co supplies are provided by the politically unstable Democratic Republic of Congo (DRC) and Zambia makes the supply unpredictable [6] with economic and supply consequences. Furthermore, the large volume of spent LIBs present hazards, such as toxic metals, organic solvents and harmful reactive inorganic compounds (e.g., $LiPF_6$ electrolyte) [7]. Regardless, the recycling rate of spent LIBs remains very low (only about 3–5%) [8,9], indicating that the current recycling processes are not easily scalable to handle the large amount of discarded LIBs every year. Therefore, the development of green, cost effective and scalable LIBs recycling processes for spent LIBs in order to protect human health and environment and support the market growth of LIBs is a necessity.

To date, hydrometallurgy, pyrometallurgy and biometallurgy are the three major recycling processes studied and used for spent LIBs. The pyrometallurgical recycling process of valuable metals from end-of-life LIBs is relatively simple and cost-effective, but it suffers from low metal recovery and atmospheric pollution issues since a large amount of hazardous gas and waste dust are generated during the thermal process [10,11]. The ''low energy'' biometallurgy process advantageously requires simple equipment. However, drawbacks such as a slow kinetics, special conditions for cultivating and storing bacteria and the need to operate with low pulp density seriously prevent the wide adoption of this method at the industrial scale [12]. Hydrometallurgy is the commonly used recycling process due to its relatively low energy consumption, low gas emission, higher metal recovery and product purity, compared to the pyrometallurgy process. The hydrometallurgical process involves acid leaching, a purification step and a metal separation step (e.g., Co from Li) either by solvent extraction or selective precipitation. Acid leaching consists of dissolving cathode active materials from the battery after mechanical treatment in common inorganic acids such as HCl, H_2SO_4, H_3PO_4 and HNO_3 [13–16]. In this process, H_2O_2 is generally used as a reducing agent to convert Co^{3+} to readily acid soluble Co^{2+} ions [17,18]. A purification step is then generally needed to remove metal impurities dissolved at the leaching step, such as Al and Cu [19]. In order to separate the metals from each other, the solvent extraction method is used. It is based on mixing the purified leaching solution with an organic extractant solution, where the extractant (e.g., Cyanex 272, Ionquest 801 or PC88A) has a specific affinity with the metal of interest so only this metal is separated from the aqueous solution and transferred to the organic phase [20–22]. The solvent extraction method generally yields high purity products but requires the usage of expensive/toxic organic chemicals and complicated experimental procedures [23,24]. In contrast, chemical precipitation, which is based on the selective precipitation of the metal of interest by adjusting the pH of the leaching solution with a precipitating agent, is scalable, simpler and more environmentally-friendly compared to the solvent extraction method [25–27]. In the literature, NaOH is typically used as the precipitating agent to recover Co as $Co(OH)_2$, while Na_2CO_3 is used to precipitate Li^+ as Li_2CO_3 [19,25]. However, the selective precipitation of $CoCO_3$ from a leaching Co/Li solution using Na_2CO_3 is poorly described in the literature.

The aim of the present article is to demonstrate the first precipitation process of sheet-like $CoCO_3$ crystals from an acid leaching solution containing Co^{2+} and Li^+ ions and to convert the sheet-like $CoCO_3$ to flower-like $LiCoO_2$ active material for reuse in LIBs. The performances of the regenerated LCO in LIB are studied and compared to those of LCO synthesized from commercial cobalt/lithium precursors. Since the use of the solvent extraction method to separate Co from the other metals is not required, the recycling process of LCO spent batteries we describe in the present manuscript is simple, environmentally-friendly and easy to process at the industrial scale.

2. Materials and Methods

2.1. Chemicals

Sulfuric acid (H_2SO_4 95%), hydrogen peroxide solution (H_2O_2, 50 wt.% in H_2O, stabilized), sodium hydroxide (NaOH, pellets, ≥97.0%), sodium carbonate powder (Na_2CO_3, ≥99.5%) and lithium carbonate (Li_2CO_3, 99.99%) were purchased from Sigma–Aldrich and used without further purification. Spent computers LCO batteries were used in this work as starting materials for cathode extraction and leaching experiments.

2.2. Pre-Treatment and Dismantling of Spent LIBs

First, the spent LIBs were completely discharged to avoid any spontaneous explosion or short-circuiting during dismantling and opening of the packaging. For discharging, spent LIBs were systematically immersed in NaOH aqueous solution and left in solution until the battery voltage became lower than 0.1 V (measured by a voltmeter). Then, the fully discharged spent LIBs were manually dismantled in order to separately collect all the components of the spent Li-ion batteries (e.g., cathode, anode, separator, packaging material, etc.) for further recycling treatment. Then, the cathode, which is composed of black material (BM) and aluminum foil, was immersed in DMF solvent and placed in an ultrasonic bath for 1 h. After being fully detached from the Al foil, the black suspension was collected using a 100 µm sieve. The BM was then separated from DMF solvent by centrifugation, washed several times with water and finally dried in air at 100 °C for further processing. The flow-sheet of the BM extraction process is shown in Figure 1.

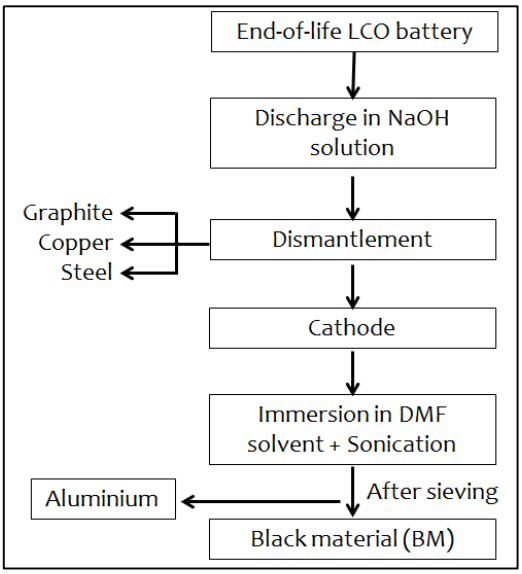

Figure 1. Flow-sheet of the black material (BM) extraction process.

2.3. Acid Leaching

The leaching step in this work was performed with H_2SO_4 in the presence of H_2O_2, used as the reducing agent to enhance the dissolution of cobalt and lithium from the black material (BM). This step was conducted in a 300 mL glass beaker put on a stirring hot plate. In a typical experiment, 10 g of BM were dispersed in 100 g of water under stirring. Then, 20 g of H_2SO_4 95% were added dropwise to the BM dispersion under vigorous stirring. The solution was then heated at 75 °C and 10 g of H_2O_2 (50 wt.% in water) were added dropwise to the mixture that was kept under stirring for 1 h. The leaching solution was finally filtered in order to separate the Co/Li leachate solution from the insoluble residue. The solid residue was washed, dried and weighed. The weight of the solid residue allowed us to calculate the dissolution efficiency (DE, in %) using the following expression:

$$DE\ (\%) = ((m_0 - m_f)/m_0) \times 100 \quad (1)$$

where DE (%) is the dissolution efficiency, m_0 is the initial weight of the BM and m_f is the weight of the dry solid residue obtained at the end of the leaching process.

The leaching efficiency of a metal × can also be calculated as follows:

$$LE_x\ (\%) = \frac{C_x^{LS} * V_{LS} + C_x^{WS} * V_{WS}}{C_x^{MS} * V_{MS} + C_x^{WS} * V_{WS} + C_x^{SR} * W_{SR}} \times 100 \quad (2)$$

where LE_x (%) is the leaching efficiency of the metal x,

$C_x{}^{LS}$: Concentration of the metal x in leaching solution (in g·L^{-1})

V_{LS}: Volume of the leaching solution (in L)

$C_x{}^{WS}$: Concentration of the metal x in the washing solution (in g·L^{-1})

V_{WS}: Volume of the washing solution (in L)

$C_x{}^{SR}$: Concentration of the metal x in the solid residue obtained at the end of the leaching process (in %)

W_{SR}: Weight of the solid residue obtained at the end of the leaching process (in g)

2.4. Purification Step

Aluminum, which is the major impurity in BM, was removed from the leaching solution by adding a 33% NaOH aqueous solution to bring the pH value up to 6.3 under stirring at about 40 °C. After 1 h stirring, the precipitate was removed by filtration and the purified solution was analyzed by inductively coupled plasma-atomic emission spectrometry (ICP-AES). The removal efficiency of Al could be assessed by calculating the precipitation efficiency (PE, in %) of Al using the following expression:

$$PE_{Al}\ (\%) = \frac{C_{Al}^{Pr} * W_{Pr}}{C_{Al}^{Pr} * W_{Pr} + C_{Al}^{LS} * V_{LS} + C_{Al}^{WS} * V_{WS}} \times 100 \quad (3)$$

where PE_{Al} (%) is the precipitation efficiency of Al

$C_{Al}{}^{Pr}$: Concentration of Al in the dry precipitate (in %)

W_{Pr}: Weight of the dry precipitate (in g)

$C_{Al}{}^{LS}$: Concentration of Al in the leachate solution (in g·L^{-1})

V_{LS}: Volume of the leachate solution (in L)

$C_{Al}{}^{WS}$: Concentration of Al in the washing solution (in g·L^{-1})

V_{WS}: Volume of the washing solution (in L)

The precipitation efficiency of Co and Li, which is not desirable at this stage, could also be calculated using the same expression.

2.5. Cobalt Recovery and Synthesis of Sheet-like Cobalt Carbonate

After the Al removal, a Co/Li-rich solution was obtained. Cobalt was then selectively precipitated from the purified solution and recovered as cobalt carbonate ($CoCO_3$). In a typical experiment, a 20% Na_2CO_3 aqueous solution was added to 100 mL of the purified Co/Li solution under vigorous stirring at 40 °C until reaching a pH = 8.2. After 45 min of stirring, the Co precipitate was filtered, washed several times with water to remove soluble salts and impurities (such as Na_2SO_4) and then dried at 80 °C for 12 h for ICP-AES measurement and further use. The reaction of $CoCO_3$ precipitation from the purified solution can be written as follows:

$$CoSO_4 + Na_2CO_3 \rightarrow CoCO_3 + Na_2SO_4 \quad (4)$$

2.6. Synthesis of Regenerated $LiCoO_2$ (LCO_{Reg}) Cathode Material

The LCO_{Reg} cathode material was successfully resynthesized by mixing the recovered $CoCO_3$ powder with Li_2CO_3 powder followed by the solid-state reaction. In a typical experiment, 0.6 g of recovered $CoCO_3$ was mixed with 0.24 g of Li_2CO_3. Then, the mixture was thoroughly mixed for 30 min using 80 mm agate mortar. The mixture was then calcined in a tubular furnace at 600 °C for 3 h and 900 °C for 10 h with a heating rate of 5 °C/min

in order to regenerate the LCO active material. The reaction of LCO formation could be written as follows:

$$4\ CoCO_3(s) + 2\ Li_2CO_3(s) + O_2(g) \rightarrow 4\ LiCoO_2(s) + 6\ CO_2(g) \quad (5)$$

The flow sheet of cobalt purification and recovery as well as the regeneration of LCO from the recovered $CoCO_3$ is shown in Figure 2.

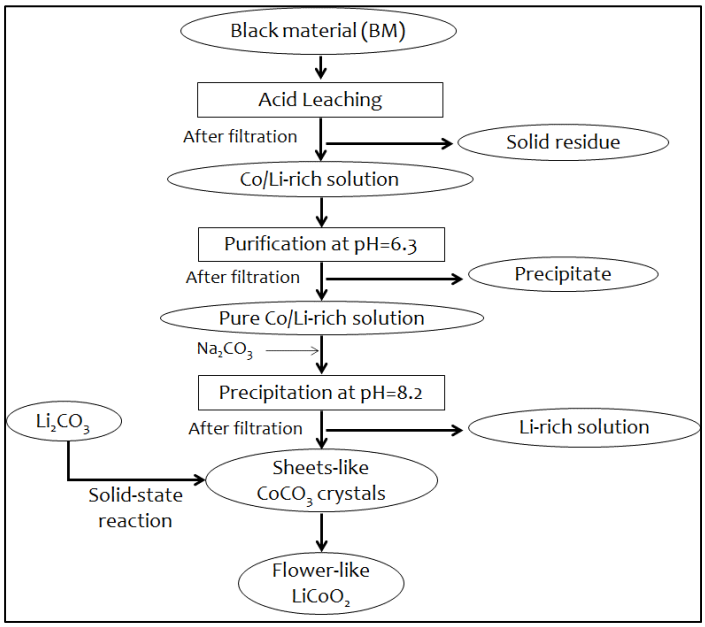

Figure 2. Flow sheet of cobalt recovery and regeneration of flower-like LCO.

2.7. Electrochemical Measurements

Electrochemical properties of the regenerated LCO from the recovered $CoCO_3$ and the synthesized LCO from the commercial $CoCO_3$ (for comparison) were assessed in CR2025 coin type cells. The cathodes were prepared by casting the slurry of the corresponding LCO on the Al foil surface using the doctor blade technique. Lithium metal was used as the anode material. The cathodes were vacuum-dried at 85 °C for 24 h. The electrolyte was 1 M $LiPF_6$ in EC + DMC (1:1 by volume). The cells were then assembled in an Ar-filled glove box, then aged for 3 h before electrochemical measurements, which were carried out between 3 V and 4.4 V (versus Li/Li^+) using a CT2001A-Land equipment under a constant current of 1C. The cells were tested over 60 charge/discharge cycles in order to characterize its cyclability and electrochemical performances. Several half-cells were systematically assembled with each LCO cathode and the electrochemical measurements were repeated thrice in order to guarantee the data accuracy and reliability. The loading weight of the LCO cathode generated from the recovered $CoCO_3$ and the LCO synthesized from commercial Li/Co precursors was 3.25 mg and 3.23 mg, respectively.

2.8. Characterization Methods

X-ray diffraction (XRD) patterns were recorded on a Bruker D8 Discover. The diffractometer was equipped with a graphite monochromator, a Lynx-Eye detector and parallel beam optics, using Cu K_α radiation (λ = 1.5418 Å). Phase identification and materials structures were determined by the HighScore software using the 2014 database. The morphology of the obtained powders was studied by scanning electron microscopy (SEM, EVO 10—with backscatter detector and element EDS system). Thermo-gravimetric analysis (TGA) of the $CoCO_3$ and the black material samples was performed using a thermal analyzer instrument (Shimadzu; model TA-60WS) under air with a heating rate of 5 °C/min. The metal content in solids and solutions was measured by ICP-AES using a 5110 ICP

AES (Agilent Technologies). In order to determine the metal concentration in the spent LCO cathode, a sample was dissolved in aqua regia solution following the experimental procedure described in the literature [28].

3. Results and Discussion

3.1. Characterization of LCO Black Material

After extraction from spent LCO batteries, the BM was fully characterized by ICP-AES, XRD, TGA and SEM techniques. Table 1 shows the chemical composition and metal content of the spent LCO cathode, as determined by ICP-AES.

Table 1. Chemical composition of the extracted LCO black material.

Element	Co	Li	Cu	Al	F
%	54.7	6.4	<0.01	0.44	0.1

ICP-AES results show that the spent LCO BM contains 54.7 wt.% cobalt and 6.4 wt.% lithium as major elements. Calculated Co/Li molar ratio is 1.01, which is very close to the theoretical molar ratio of 1.00 in $LiCoO_2$. The BM sample also includes 0.44% Al and 0.1% F, due to the residual $LiPF_6$ electrolyte (and eventually PVDF binder), as minor constituents. The total weight of Co, Li, Al and F corresponds to about 96% in weight of the BM sample, which suggests that the remaining 4 wt.% constituent is likely carbon-based compounds and/or residual PVDF, commonly used as a conductive material and/or a binder during the preparation of the LCO active material. This assumption was confirmed by the TGA analysis of the BM (Figure S1, Supplementary Materials) which clearly shows a weight loss of about 4.3% between about 300 °C and 700 °C due to the decomposition of the carbon-based compounds present in the BM, in agreement with the reported data [29].

The BM was also characterized by XRD and SEM as shown in Figure 3. The XRD analysis indicates the presence of the hexagonal crystalline structure of lithium cobalt oxide (JCPDS n° 96-450-5483). The XRD pattern of BM doesn't reveal the presence of other crystalline compounds, which suggests that the carbon-based compounds present in the BM are amorphous. The SEM images recorded on the BM sample revealed the formation of micro-sized particles with irregular size and shape as shown in Figure 3a.

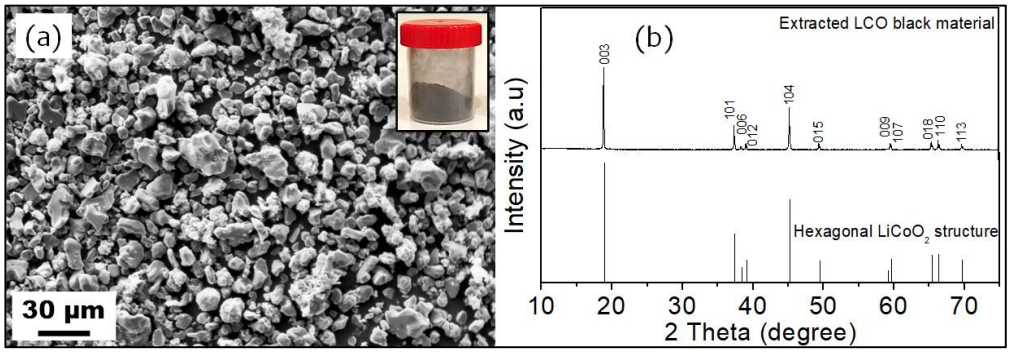

Figure 3. SEM image (**a**) and XRD pattern (**b**) of the extracted BM. The inset of figure (**a**) is a digital photograph of the extracted BM.

3.2. Acid Leaching of Co and Li from BM

Performances of the acid leaching conducted with sulfuric acid and H_2O_2 (used as reducing agent) are given in Table 2. Results showed that over 99% of Co and almost the totality of Li and Al were dissolved in solution, resulting in high Co and Li concentration in the leaching solution (25.42 $g{\cdot}L^{-1}$ and 3.2 g/L^{-1} of Co and Li, respectively). Although, the Al concentration is low (0.13 $g{\cdot}L^{-1}$), the removal of this impurity from the leaching solution is mandatory in order to achieve a high purity $CoCO_3$ precursor during the precipitation step.

Table 2. Leaching efficiency (LE) in %, dissolution efficiency (DE) in % and concentration of each metal in the leaching solution (LS) in $g \cdot L^{-1}$.

Element	Co	Li	Al
Concentration in LS ($g \cdot L^{-1}$)	25.42	3.20	0.13
LE (%)	99.1	99.9	99.8
DE (%)	96		

Results also showed that about 96% of the BM sample is dissolved in the leaching medium, which is in agreement with the TGA result (Figure S1). The leaching residue that accounts for about 4% in weight of the initial black material was also analyzed by XRD (Figure S3, Supplementary Materials) which clearly shows that the remaining materials after leaching are graphite and carbon. The XRD pattern of the residue also indicates the absence of LCO peaks and confirms the full extraction of Li and Co from the spent LCO BM.

3.3. Purification Step (Removal of Al Impurities from the Leaching Solution)

ICP-AES results showed that over 90% Al impurities were successfully removed from the leaching solution at pH = 6.3, as shown in Table 3. We should note that Co and Li concentration in the purified solution is lower than the initial concentration in LS due to the dilution effect resulting from the addition of the 33% NaOH solution and not from their precipitation since the PE (%) of Co and Li at this pH is low (1.7% and 2.5%, respectively). Nevertheless, Co concentration (17.9 $g \cdot L^{-1}$) is still high in the purified solution and even much higher than the typical Co concentration in standard Co hydrometallurgy plants where the high grades Cu ores, from which Co is produced as a by-product, generally provide about 3 g of Co per L [30]. After purification, the Co/Li solution contains only 0.01 $g \cdot L^{-1}$ Al, which is much lower when compared to the un-purified leaching solution.

Table 3. Results of the purification step to remove Al from the leaching solution.

Element	Co	Li	Al
Concentration in purified solution ($g \cdot L^{-1}$)	17.90	2.10	0.01
PE (%)	1.7	2.5	90.1

3.4. Cobalt Recovery and Synthesis of Sheet-like Cobalt Carbonate

Cobalt is recovered as a carbonate, $CoCO_3$, with a precipitation yield higher than 99% as shown in Table 4. Interestingly, precipitation efficiency of Li at this stage is low (3.2% only), which allowed us to achieve high grade $CoCO_3$ product. Cobalt content in $CoCO_3$ determined by ICP-AES is 48.2% (w/w), which is close to the theoretical value of 49.5% (w/w) and satisfies the commercial standard requirements for this product in the industry (47–48% w/w of Co content). This result is also supported by the TGA measurement (Figure S2, Supplementary Materials) indicating a total weight loss of 32.7% between 100 °C and 500 °C, due to the thermal decomposition of $CoCO_3$ to Co_3O_4, which is very close to the theoretical value of 33.06% and thus confirms the high purity of the recovered $CoCO_3$ product. Moreover, the Li content in $CoCO_3$ is low (only 0.18% w/w) and should not compromise the re-synthesis of a new $LiCoO_2$ cathode material since it is one of this compound-forming element. In addition, the recovered Co precipitate has a red/pink color, which is characteristic of $CoCO_3$, as shown in the inset of Figure 4b.

The recovered $CoCO_3$ was also characterized by SEM and XRD in order to investigate the morphology and the crystalline structure of this material. Results are presented in Figure 4.

The XRD pattern of $CoCO_3$ fits well with the major peaks of the hexagonal $CoCO_3$ crystalline structure of spherocobaltite (JCPDS card number 96-900-7714) and shows that no other chemical component is present in the sample, which is in agreement with ICP-

AES and TGA results. Interestingly, the SEM image (Figure 4a) shows that the $CoCO_3$ crystals exhibit a sheet-like morphology with relatively uniform shape and size. The high magnification SEM image (inset of Figure 4a) shows that the $CoCO_3$ crystals have a thickness of about 100–150 nm and a diameter around 10–15 µm. The low thickness of $CoCO_3$ sheets is in agreement with the broadening of XRD peaks observed in the XRD pattern of the sample (Figure 4b).

Table 4. Results of the selective precipitation of Co at pH = 8.2.

Element	Co	Li
Concentration in the purified solution ($g \cdot L^{-1}$)	17.9	2.1
Concentration in the precipitate of pH = 8.2 (%)	48.20	0.18
PE (%)	99.2	3.2

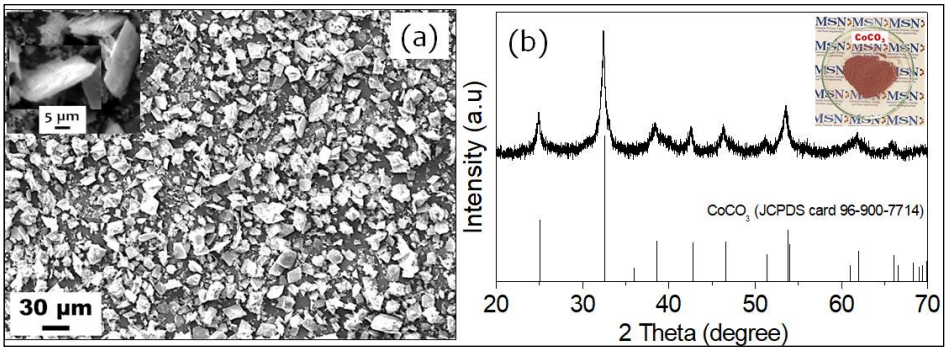

Figure 4. SEM image with two different magnifications (**a**) and XRD pattern (**b**) of recovered $CoCO_3$. The inset of (**b**) shows a digital photograph of the dried $CoCO_3$ powder.

3.5. Regeneration of $LiCoO_2$ (LCO_{Reg}) from the Recovered Sheet-like $CoCO_3$ and Its Electrochemical Performances

As described above, the sheet-like $CoCO_3$ powder was thoroughly mixed with Li_2CO_3 in order to regenerate $LiCoO_2$ (LCO_{Reg}) by the high temperature solid-state method. For comparison purposes, $LiCoO_2$ prepared from commercial $CoCO_3$ and Li_2CO_3 (LCO_{Com}) was also synthesized, using the same synthesis method. At first, XRD and SEM analysis were conducted on the resulting LCO_{Reg} solid in order to characterize its structure and morphology. Results are provided in Figure 5.

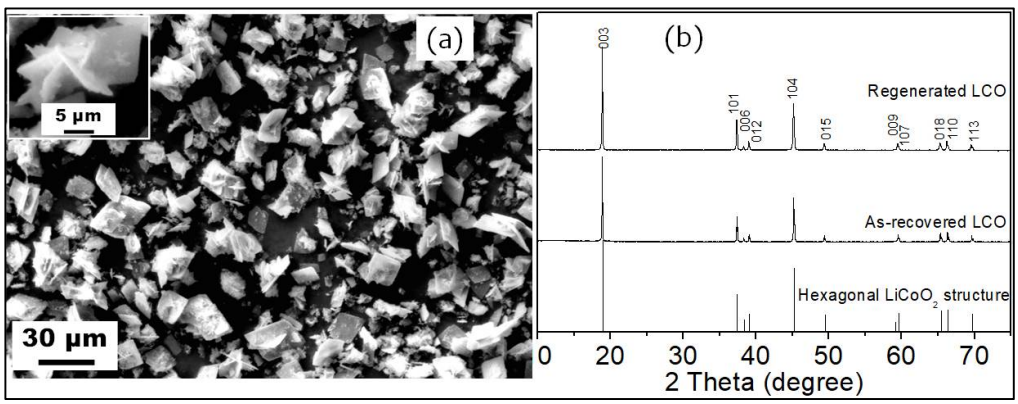

Figure 5. (**a**) SEM image with two different magnifications of $LiCoO_2$ regenerated from sheet-like $CoCO_3$ (LCO_{Reg}) and (**b**) XRD pattern of LCO_{Reg} and LCO synthesized from commercial $CoCO_3$ (LCO_{Com}).

The SEM images clearly show that the starting $CoCO_3$ "flakes", used as Co precursor to synthesize LCO_{Reg}, were conjugated to each other and formed a flower-like LCO structure after the solid-state reaction, as demonstrated by the inset of Figure 5a. For comparison with LCO_{Reg} cathode, the SEM picture of LCO_{Com} is also provided in Figure S4 (Supplementary Materials). As shown by Figure S4, LCO_{Com} exhibits grains with irregular shape and large particle size in the range of 10–25 µm. Results also show that both LCO_{Reg} and LCO_{Com} have similar XRD patterns that fit with the hexagonal $LiCoO_2$ structure as demonstrated in Figure 5b. XRD peaks are also significantly narrow and intense, which indicate that both materials are highly crystalline. The crystallite size calculated from the broadening of XRD peaks using the Debye-Scherrer equation is about 80 nm and 90 nm for LCO_{Reg} and LCO_{Com}, respectively.

The electrochemical behavior of both LCO_{Reg} and LCO_{Com} cathodes in the half-cells was also investigated and results are provided in Figure 6.

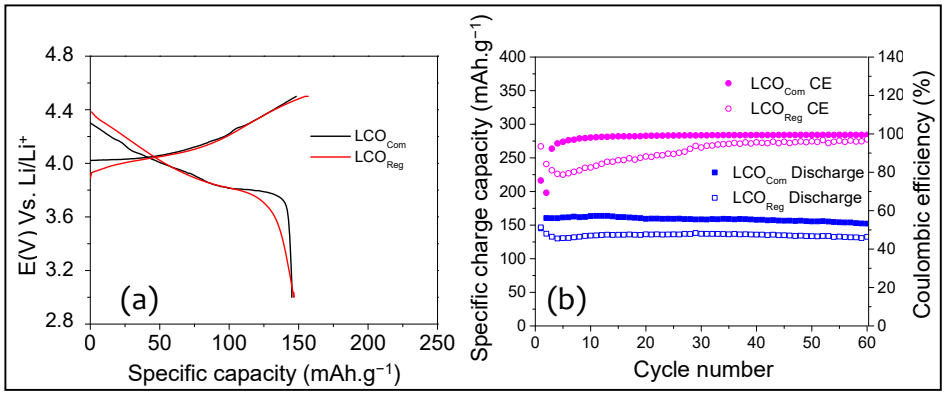

Figure 6. First charge/discharge curve (**a**), cycling performance and coulombic efficiency (CE) (**b**) of LCO_{Reg} and LCO_{Com} cathodes in Li-ion half-cells.

Results show that LCO_{Reg} has an initial discharge specific capacity of about 146 $mAh.g^{-1}$ at 1C rate with an initial coulombic efficiency of 93%, which is relatively comparable to LCO_{Com}. The initial discharge capacity of LCO_{Reg} is also roughly similar to most reported data of regenerated $LiCoO_2$ cathodes in the literature, although a strict comparison could not be made as the measurement conditions (voltage range, current rate (C), electrolyte concentration and composition, cathode preparation, etc.) differ from one study to another [31–33]. Moreover, like LCO_{Com}, the LCO_{Reg} cathode material exhibits stable cycling performances with a capacity retention of 90% after 60 cycles and a coulombic efficiency of about 96%, which suggests that the regenerated cathode has a stable and robust crystalline structure. This result is also supported by the cyclic voltammetry (CV) measurements performed on the Li/LCO half-cells of LCO_{Reg} and LCO_{Com} cathodes (Figure S5, Supplementary Materials) which showed relatively stable and characteristic LCO CV curves for both LCO_{Reg} and LCO_{Com} cathodes [34]. Interestingly, the potential difference between the oxidation and the reduction peaks (ΔV) was found to be lower in the case of LCO_{Reg}, compared to LCO_{Com}, reflecting a faster lithiation/delithiation kinetics with the regenerated LCO cathode. These results indicate that this simple recycling process provides cobalt carbonate with properties comparable to those of commercial cobalt precursors and thus could be successfully used to restore LCO cathode materials from spent LIBs. This process is advantageously simple and environmentally-friendly since the use of solvent extraction method is not required. Recovery of Li from the Li-rich solution (shown in Figure 2) is currently under optimization and results will be published in the near future.

4. Conclusions

This work proposes a simple hydrometallurgy process for recycling cobalt from spent LCO LIBs and its purification and separation from lithium without using the complicated solvent extraction method and the related toxic and expensive organic substances. The method is based on the acid leaching of the black material in H_2SO_4/H_2O_2 aqueous solution, the removal of Al impurity at pH = 6.2 and the selective precipitation of Co at pH = 8.2 using an aqueous solution of Na_2CO_3. The overall recovery rate of Co by this method (including leaching, purification and precipitation steps) is higher than 96%. The method yielded a high grade $CoCO_3$ (48.2% Co, *w*/*w*), containing only 0.18% Li, which makes the product highly suitable for re-use in manufacturing a fresh LCO cathode material. SEM observations revealed that the recovered $CoCO_3$ has a unique sheet-like structure with a relatively uniform diameter. The recovered $CoCO_3$ was used to regenerate LCO powder with a flower-like morphology through a solid-state reaction using Li_2CO_3 as the Li precursor. The regenerated LCO cathode displayed an initial discharge capacity that is roughly similar to the LCO prepared from the commercial Co/Li precursors with capacity retention of 90% at the 60th cycle. Considering the context of the current rise in cobalt prices and the high commercial value of $CoCO_3$ prepared in the present work, recycling Co from spent LIBs using this simple process is economically attractive.

Supplementary Materials: The following supporting information can be downloaded at: https://www.mdpi.com/article/10.3390/su14052552/s1. Figure S1: TGA curve of as-extracted LCO black material. Figure S2: TGA curve of sheet-like cobalt carbonate ($CoCO_3$) recovered from spent LCO battery. Figure S3: XRD pattern of the leaching solid residue resulting from the acid leaching step. Figure S4: SEM image of LCO_{Com} synthesized from commercial Li/Co precursors using solid-state method. Figure S5: Cyclic voltammograms of LCO_{Reg} and LCO_{Com}.

Author Contributions: Conceived the research idea and designed the experiments, A.A.; Performed the experiments together, A.Y. and N.E.; Prepared the cathodes for LIB testing, M.T.; Performed the XRD analysis, M.A.; Performed the electrochemical measurements and analyzed the data, L.H.; Reviewed the article and validated its scientific content, M.D. and J.A. All authors have read and agreed to the published version of the manuscript.

Funding: This research received no external funding.

Institutional Review Board Statement: Not applicable.

Informed Consent Statement: Not applicable.

Data Availability Statement: Not applicable.

Acknowledgments: The authors thank Aziz Soulaimani and Sabah Fathallah (UM6P) for ICP-AES measurements.

Conflicts of Interest: The authors declare no conflict of interest.

References

1. Projected Size of the Global Lithium-Ion Battery Market from 2020 to 2026. Available online: https://www.statista.com/statistics/1011187/projected-global-lithium-ion-battery-market-size/ (accessed on 21 November 2021).
2. Shen, C.; Wang, H. Research on the technological development of lithium ion battery industry in China. *J. Phys. Conf. Ser.* **2019**, *1347*, 012087. [CrossRef]
3. Zeng, X.; Li, J. Implications for the carrying capacity of lithium reserve in China. *Resour. Conserv. Recycl.* **2013**, *80*, 58–63. [CrossRef]
4. Gao, W.; Liu, C.; Cao, H.; Zheng, X.; Lin, X.; Wang, H.; Zhang, Y.; Sun, Z. Comprehensive evaluation on effective leaching of critical metals from spent lithium-ion batteries. *Waste Manag.* **2018**, *75*, 477–485. [CrossRef]
5. Trading Economics: Cobalt. Available online: https://tradingeconomics.com/commodity/cobalt (accessed on 21 November 2021).
6. Olivetti, E.A.; Ceder, G.; Gaustad, G.G.; Fu, X. Lithium-ion battery supply chain considerations: Analysis of potential bottlenecks in critical metals. *Joule* **2017**, *1*, 229–243. [CrossRef]
7. Yu, Y.; Chen, B.; Huang, K.; Wang, X.; Wang, D. Environmental impact assessment and end-of-life treatment policy analysis for Li-ion batteries and Ni-MH batteries. *Int. J. Environ. Res. Public Health* **2014**, *11*, 3185–3198. [CrossRef]
8. Natarajan, S.; Aravindan, V. Recycling strategies for spent Li-ion battery mixed cathodes. *ACS Energy Lett.* **2018**, *3*, 2101–2103. [CrossRef]

9. Sonoc, A.; Jeswiet, J.; Soo, V.K. Opportunities to improve recycling of automotive lithium ion batteries. *Procedia Cirp.* **2015**, *29*, 752–757. [CrossRef]
10. Georgi-Maschler, T.; Friedrich, B.; Weyhe, R.; Heegn, H.; Rutz, M. Development of a recycling process for Li-ion batteries. *J. Power Sources* **2012**, *207*, 173–182. [CrossRef]
11. Lv, W.; Wang, Z.; Cao, H.; Sun, Y.; Zhang, Y.; Sun, Z. A critical review and analysis on the recycling of spent lithium-ion batteries. *ACS Sustain. Chem. Eng.* **2018**, *6*, 1504–1521. [CrossRef]
12. Zhuang, W.-Q.; Fitts, J.P.; Ajo-Franklin, C.M.; Maes, S.; Alvarez-Cohen, L.; Hennebel, T. Recovery of critical metals using biometallurgy. *Curr. Opin. Biotechnol.* **2015**, *33*, 327–335. [CrossRef]
13. Lee, C.K.; Rhee, K.-I. Reductive leaching of cathodic active materials from lithium ion battery wastes. *Hydrometallurgy* **2003**, *68*, 5–10. [CrossRef]
14. Pinna, E.G.; Ruiz, M.C.; Ojeda, M.W.; Rodriguez, M.H. Cathodes of spent Li-ion batteries: Dissolution with phosphoric acid and recovery of lithium and cobalt from leach liquors. *Hydrometallurgy* **2017**, *167*, 66–71. [CrossRef]
15. Wang, R.-C.; Lin, Y.-C.; Wu, S.-H. A novel recovery process of metal values from the cathode active materials of the lithium-ion secondary batteries. *Hydrometallurgy* **2009**, *99*, 194–201. [CrossRef]
16. Aaltonen, M.; Peng, C.; Wilson, B.P.; Lundström, M. Leaching of metals from spent lithium-ion batteries. *Recycling* **2017**, *2*, 20. [CrossRef]
17. Zhu, S.-g.; He, W.-Z.; Li, G.-M.; Xu, Z.; ZHANG, X.-j.; Huang, J.-W. Recovery of Co and Li from spent lithium-ion batteries by combination method of acid leaching and chemical precipitation. *Trans. Nonferrous Met. Soc. China* **2012**, *22*, 2274–2281. [CrossRef]
18. Kang, J.; Senanayake, G.; Sohn, J.; Shin, S.M. Recovery of cobalt sulfate from spent lithium ion batteries by reductive leaching and solvent extraction with Cyanex 272. *Hydrometallurgy* **2010**, *100*, 168–171. [CrossRef]
19. Wang, H.; Vest, M.; Friedrich, B. Hydrometallurgical processing of Li-Ion battery scrap from electric vehicles. In Proceedings of the 6th European Metallurgical Conference (EMC), Santa Barbara, CA, USA, 22–24 June 2011.
20. Swain, B.; Jeong, J.; Lee J-c Lee, G.-H.; Sohn, J.-S. Hydrometallurgical process for recovery of cobalt from waste cathodic active material generated during manufacturing of lithium ion batteries. *J. Power Sources* **2007**, *167*, 536–544. [CrossRef]
21. Pranolo, Y.; Zhang, W.; Cheng, C. Recovery of metals from spent lithium-ion battery leach solutions with a mixed solvent extractant system. *Hydrometallurgy* **2010**, *102*, 37–42. [CrossRef]
22. Nan, J.; Han, D.; Yang, M.; Cui, M.; Hou, X. Recovery of metal values from a mixture of spent lithium-ion batteries and nickel-metal hydride batteries. *Hydrometallurgy* **2006**, *84*, 75–80. [CrossRef]
23. Gaines, L. Lithium-ion battery recycling processes: Research towards a sustainable course. *Sustain. Mater. Technol.* **2018**, *17*, e00068. [CrossRef]
24. Zhou, L.-F.; Yang, D.; Du, T.; Gong, H.; Luo, W.-B. The current process for the recycling of spent lithium ion batteries. *Front. Chem.* **2020**, *8*, 578044. [CrossRef] [PubMed]
25. Contestabile, M.; Panero, S.; Scrosati, B. A laboratory-scale lithium-ion battery recycling process. *J. Power Sources* **2001**, *92*, 65–69. [CrossRef]
26. Dorella, G.; Mansur, M.B. A study of the separation of cobalt from spent Li-ion battery residues. *J. Power Sources* **2007**, *170*, 210–215. [CrossRef]
27. Li, J.; Shi, P.; Wang, Z.; Chen, Y.; Chang, C.-C. A combined recovery process of metals in spent lithium-ion batteries. *Chemosphere* **2009**, *77*, 1132–1136. [CrossRef] [PubMed]
28. Xiao, X.; Hoogendoorn, B.W.; Ma, Y.; Sahadevan, S.A.; Gardner, J.M.; Forsberg, K.; Olsson, R.T. Ultrasound-assisted extraction of metals from Lithium-ion batteries using natural organic acids. *Green Chem.* **2021**, *23*, 8519–8532. [CrossRef]
29. Zheng, Y.; Song, W.; Mo, W.-t.; Zhou, L.; Liu, J.-W. Lithium fluoride recovery from cathode material of spent lithium-ion battery. *RSC Adv.* **2018**, *8*, 8990–8998. [CrossRef]
30. Sole, K.C.; Parker, J.; Cole, P.M.; Mooiman, M.B. Flowsheet options for cobalt recovery in African copper–cobalt hydrometallurgy circuits. *Miner. Processing Extr. Metall. Rev.* **2019**, *40*, 194–206. [CrossRef]
31. Sita, L.E.; da Silva, S.P.; da Silva, P.R.C.; Scarminio, J. Re-synthesis of $LiCoO_2$ extracted from spent Li-ion batteries with low and high state of health. *Mater. Chem. Phys.* **2017**, *194*, 97–104. [CrossRef]
32. Tang, Y.; Xie, H.; Zhang, B.; Chen, X.; Zhao, Z.; Qu, J.; Xing, P.; Yin, H. Recovery and regeneration of $LiCoO_2$-based spent lithium-ion batteries by a carbothermic reduction vacuum pyrolysis approach: Controlling the recovery of CoO or Co. *Waste Manag.* **2019**, *97*, 140–148. [CrossRef]
33. Li, L.; Chen, R.; Sun, F.; Wu, F.; Liu, J. Preparation of $LiCoO_2$ films from spent lithium-ion batteries by a combined recycling process. *Hydrometallurgy* **2011**, *108*, 220–225. [CrossRef]
34. Guo, H.-L.; Lin, H.-F.; Yang, Y.-C.; Cheng, C.-H.; Tsai, Y.-R.; Wang, F.-M. Modification of $LiCoO_2$ through rough coating with lithium lanthanum zirconium tantalum oxide for high-voltage performance in lithium ion batteries. *J. Solid State Electrochem.* **2021**, *25*, 105–115. [CrossRef]